

Quantification of Vibration Localization in Periodic Structures

A. Chandrasher

College of Engineering,
Swansea University,
Swansea SA1 8EN, UK

S. Adhikari¹

College of Engineering,
Swansea University,
Swansea SA1 8EN, UK
e-mail: s.adhikari@swansea.ac.uk

M. I. Friswell

College of Engineering,
Swansea University,
Swansea SA1 8EN, UK

The phenomenon of vibration mode localization in periodic and near periodic structures has been well documented over the past four decades. In spite of its long history, and presence in a wide range of engineering structures, the approach to detect mode localization remains rather rudimentary in nature. The primary way is via a visual inspection of the mode shapes. For systems with complex geometry, the judgment of mode localization can become subjective as it would depend on visual ability and interpretation of the analyst. This paper suggests a numerical approach using the modal data to quantify mode localization by utilizing the modal assurance criterion (MAC) across all the modes due to changes in some system parameters. The proposed MAC localization factor (MACLF) gives a value between 0 and 1 and therefore gives an explicit value for the degree of mode localization. First-order sensitivity based approaches are proposed to reduce the computational effort. A two-degree-of-freedom system is first used to demonstrate the applicability of the proposed approach. The finite element method (FEM) was used to study two progressively complex systems, namely, a coupled two-cantilever beam system and an idealized turbine blade. Modal data is corrupted by random noise to simulate robustness when applying the MACLF to experimental data to quantify the degree of localization. Extensive numerical results have been given to illustrate the applicability of the proposed approach. [DOI: 10.1115/1.4032032]

1 Introduction

Structures with uniform periodic spacing and repeated geometry are found in complex engineering systems. Examples include turbine blades, ship hull, aircraft fuselage, and oil pipelines with periodic supports [1]. The vibration characteristics of these periodic structures are highly sensitive to its mass distribution, stiffness distribution, and geometrical properties. Parametric uncertainties in structures which arise due to material defects, structural damage, or variations in material properties can break the symmetry of periodic structures. These uncertainties can drastically change and localize different vibration modes. Identification of severe mode localization in the design process can help prevent failure due to high cycle fatigue (HCF) in periodic structures such as turbine blades. Mode localizations are often directly detected by simple visual means, such as by looking at the animation of mode shapes given by a finite element software. Although a visual approach is physically intuitive, in some cases (e.g., complex geometry) the identification of mode localization can be subjective and may not be obvious. A numerical approach may provide a solution by removing or substantially reducing the need for a subjective opinion about the localization. The purpose of this paper is to suggest a numerical approach using the modal data toward achieving this objective. The proposed numerical approach can be used independently or in conjunction with the visual inspection of standard mode shape plots.

Numerous examples of linearly and rotationally periodic structures can be found in many Aerospace, Civil, and Mechanical engineering applications such as turbine blades, Aircraft fuselages, and oil pipe lines with periodic supports. Excitation of the localized vibration modes can lead to HCF which contributes to premature failure of the structure [2,3]. HCF in turbine blades has been identified as the major cause of Aircraft Engine failures [3]. Perfect periodic structures are idealized cases while in reality

most structures are only nearly periodic due to parametric uncertainties such as material imperfections or structural damage. As structures are not perfectly periodic, various authors have introduced intentional mistuning to reduce the effects of localization in turbine blades. Castanier and Pierre [2] discussed the importance of preventing HCF and summarized the design strategies used thus far to prevent extreme localization. An excellent review in Refs. [3,4] can be referred for more details about intentional mistuning and reduction of the forced response of bladed disks. Blair [5] proposed disk modifications to find the configuration that would give the best mistuning pattern using the FEM. More recently, Chen and Shen [6] provided useful mathematical insights into linear mode localization in nearly cyclic symmetric rotors with mistune.

Early works on periodic or near-periodic structures used the transfer matrix method [7]. Soong and Bogdanoff [8] used the transfer matrix method to study the statistics of disordered spring-mass chains of N degrees-of-freedom. Lin and Yang [9] determined the random natural frequencies of a disordered periodic beam. A first-order perturbation procedure was used to derive expressions of variances of natural frequencies and normal modes for different cases of random bending stiffness and span lengths. The natural frequencies were found to be more sensitive to span variation than to bending stiffness fluctuation. Yang and Lin [10] also studied the mean and variance of the frequency response function of a disordered periodic beam using the transfer matrix method. Kissel [11,12], Lin and Cai [13], Lin and Cai [14], Xie and Ariaratnam [15–17], and Ariaratnam and Xie [18] used transfer matrices in the context of randomly disordered periodic structures within the framework of wave propagation analysis under the assumption that spatial disorder is modeled as an ergodic random process. Fang [19] combined transfer matrix methods with the first-order second moment approach to analyze the natural frequencies and mode-shapes of uncertain beam structures. As an example a cantilever beam is considered and divided into five segments with third and fifth segments have uncertainties in mass and Young's modulus, respectively. A computational algorithm based on transfer matrices to compute natural frequencies of a fixed-fixed string with a set of intermediate random spring

¹Corresponding author.

Contributed by the Technical Committee on Vibration and Sound of ASME for publication in the JOURNAL OF VIBRATION AND ACOUSTICS. Manuscript received April 7, 2015; final manuscript received November 12, 2015; published online January 18, 2016. Assoc. Editor: Jeffrey F. Rhoads.

supports has been outlined by Mitchell and Moini [20]. Langley [21] used transfer matrices for vibration energy flow analysis of structures. It was shown that the transfer matrix which governs harmonic motion in a conservative system is K-unitary.

Although the transfer matrix method has been used successfully to understand the response statistics of randomly disordered periodic structures, it is inconvenient to predict mode localization using this approach. It can be extremely difficult and tedious to individually observe all the vibration modes when making a number of design changes to the system. The veering phenomena [22], where the eigenvalues are plotted against a varying design parameter, can be used to detect the localized modes [2,23]. A numerical approach to quantify mode veering has been proposed recently [24], which largely eliminates the need to identify mode veering using the conventional visual approach. A method to numerically identify mode localization could provide similar benefit. For periodic structures, spatial mode localization is often associated with a pair of closely spaced natural frequencies. Therefore, by calculating the correlation of the modal vectors corresponding to system natural frequencies can provide a numerical way to identify mode localization. This paper proposes such a method based on the MAC [25]. This may help designers to easily obtain crucial information such as the degree of localization for all the vibration modes in the system.

In Sec. 3, an approach to quantify mode localization using the MAC is proposed. A simple two degrees-of-freedom (2DOF) system is used to illustrate mode localization and a more complex coupled cantilever system is chosen to numerically study a linearly periodic system possessing distinct eigenvalues. To demonstrate a rotationally periodic system with repeated eigenvalues the bladed disk system was used as an example in Sec. 5. The proposed MACLF for the modes under consideration is shown using the coupled cantilever system and the bladed disk system. For large systems first-order sensitivity methods are utilized to calculate the eigenvalues and eigenvectors for variations in the system design parameters. The sensitivity of a bladed disk system to the changes in the mass and stiffness matrix was simulated by (a) varying the mass distribution and (b) varying the stiffness distribution. In both cases, the localization of vibration is observed. The MACLF is applied to the two numerical studies, and its effectiveness is verified by curve veering and inspection of the mode shapes. To simulate realistic experimental conditions, numerical noise is also added to the modal data and the sensitivity of MACLF to noise is shown in Sec. 5.3. A set of conclusions drawn based on this study is summarized in Sec. 6.

2 Background of Mode Veering

The general eigenvalue equation of a linear undamped system with N degrees-of-freedom is

$$[\mathbf{K}(\mathbf{p}) - \lambda_j \mathbf{M}(\mathbf{p})] \mathbf{x}_j = 0 \quad (1)$$

where \mathbf{M} and $\mathbf{K} \in \mathbb{R}^{N \times N}$ are the mass and stiffness matrices, and λ_j and $\mathbf{x}_j \in \mathbb{R}^N$ are the eigenvalues and eigenvectors of the dynamic system. The subscript $j \in [1, 2, \dots, N]$ represents the mode number of the system. Parametric uncertainties in a system can be modeled as functions of the parameter vector \mathbf{p} , where \mathbf{p} could be the material or geometrical properties of the physical system. A 2DOF system illustrated in Fig. 1 has only two possible modes, namely, the first mode where m_1 and m_2 oscillate in phase and the second mode where the masses oscillate out of phase.

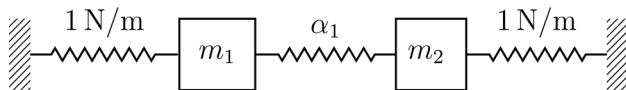


Fig. 1 The 2DOF spring–mass system

Pierre [26] showed that weak coupling can localize the vibration modes. Vibrations can also be localized when the mass distribution in the system is disturbed. For example, assume that the system illustrated in Fig. 1 is undamped, and that $m_1 = 1$ kg and $m_2 = \epsilon m_1$. Then the generalized eigenvalue equation becomes

$$\begin{bmatrix} 1 + \alpha_1 - \lambda_j & -\alpha_1 \\ -\alpha_1 & \alpha_1 + 1 - \lambda_j \epsilon \end{bmatrix} \begin{Bmatrix} x_{1j} \\ x_{2j} \end{Bmatrix} = 0 \quad (2)$$

where $\mathbf{x}_j = \begin{Bmatrix} x_{1j} \\ x_{2j} \end{Bmatrix}$. The eigenvalues may be calculated as

$$\begin{aligned} \lambda_1 &= \frac{-\epsilon(\alpha_1 - 1) - \alpha_1 - 1 + \sqrt{\epsilon^2 \phi + 2\epsilon\gamma + \phi}}{-2\epsilon} \\ \lambda_2 &= \frac{\epsilon(1 + \alpha_1) + \alpha_1 + 1 + \sqrt{\epsilon^2 \phi + 2\epsilon\gamma + \phi}}{2\epsilon} \end{aligned} \quad (3)$$

where $\phi = \alpha_1^2 + 2\alpha_1 + 1$ and $\gamma = \alpha_1^2 - 2\alpha_1 - 1$ represent the quadratic terms of coupling α_1 . The corresponding mass normalized eigenvectors, \mathbf{x}_1 and \mathbf{x}_2 , are

$$\begin{aligned} \mathbf{x}_1 &= \frac{1}{\sqrt{1 + \frac{(-\lambda_1 + 1 + \alpha_1)^2 \epsilon}{\alpha_1^2}}} \begin{Bmatrix} -\lambda_1 + 1 + \alpha \\ \alpha_1 \end{Bmatrix} \\ \mathbf{x}_2 &= \frac{1}{\sqrt{1 + \frac{(-\lambda_2 + 1 + \alpha_1)^2 \epsilon}{\alpha_1^2}}} \begin{Bmatrix} -\lambda_2 + 1 + \alpha \\ \alpha_1 \end{Bmatrix} \end{aligned} \quad (4)$$

Figure 2 shows the change in eigenvalues and eigenvectors obtained by perturbing the mass matrix by ϵ in the presence of weak coupling ($\alpha_1 = 0.1 \text{ N m}^{-1}$). The closely spaced eigenvalues are shown to veer for a variation in ϵ . Figure 2 shows that \mathbf{a}_j , \mathbf{b}_j , and \mathbf{c}_j represent the eigenvectors of the 2DOF system for $\epsilon = 0.25, 1$, and 1.55 , respectively. The vectors may be computed as

$$\begin{aligned} \mathbf{a}_1 &= \begin{Bmatrix} 0.99 \\ 0.12 \end{Bmatrix}, & \mathbf{b}_1 &= \begin{Bmatrix} 0.70 \\ 0.70 \end{Bmatrix}, & \mathbf{c}_1 &= \begin{Bmatrix} 0.19 \\ 0.78 \end{Bmatrix} \\ \mathbf{a}_2 &= \begin{Bmatrix} 0.06 \\ -1.99 \end{Bmatrix}, & \mathbf{b}_2 &= \begin{Bmatrix} 0.70 \\ -0.70 \end{Bmatrix}, & \mathbf{c}_2 &= \begin{Bmatrix} 0.98 \\ -0.15 \end{Bmatrix} \end{aligned} \quad (5)$$

At the extreme ends of the curve veering region in Figure 2(a) (\mathbf{a}_j and \mathbf{c}_j), the vibrations are confined to one region, whereas the eigenvectors \mathbf{b}_j indicate evenly distributed vibrations. For a simple system, the eigenvectors can be examined to detect localization but for realistic finite element models such as a bladed disk system with 100,000 or more degrees-of-freedom, it would be impossible to quantify localization. For a more complex system, the changes in the mass and stiffness distribution can localize its modes with different levels of severity. Fox and Kapoor [27] derived a first-order expression for the derivative of eigenvectors with distinct eigenvalues for undamped systems. Equivalent expressions for viscously damped [28] as well nonviscously [29] damped systems are also available in literature. For a variation of m_2 , the derivative of the mass and stiffness matrices for the 2DOF system illustrated in Fig. 2 is

$$\frac{\partial \mathbf{M}}{\partial m_2} = \begin{bmatrix} 0 & 0 \\ 0 & 1 \end{bmatrix}, \quad \frac{\partial \mathbf{K}}{\partial m_2} = 0 \quad (6)$$

which gives the derivative of Mode 1 as

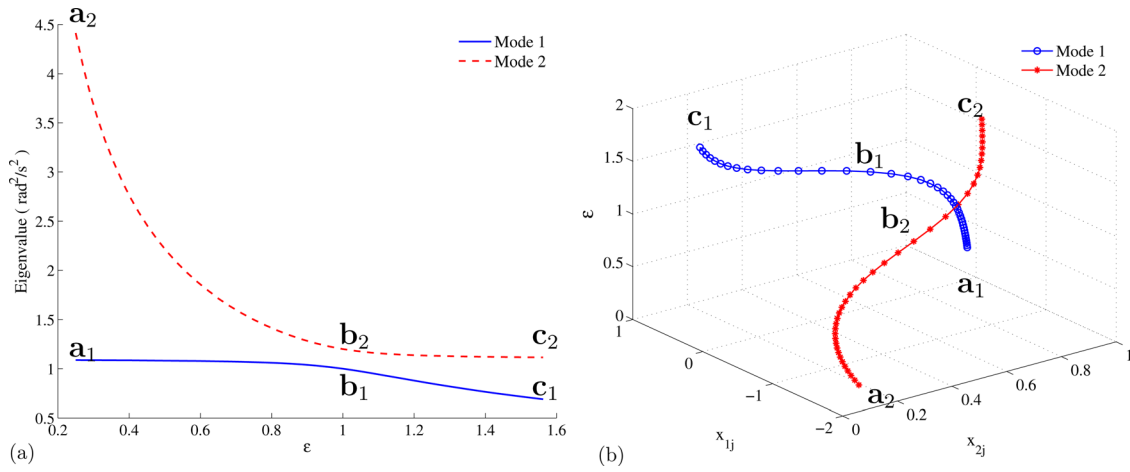


Fig. 2 Eigenvalue veering and mode localization in the 2DOF discrete spring–mass system for a variation in $m_2 = \epsilon m_1$ and $\alpha_1 = 0.1$: (a) Eigenvalue veering and (b) eigenvectors

$$\frac{\partial \mathbf{x}_1}{\partial m_2} = \left\{ \begin{array}{l} -\frac{1}{2} \frac{(-\lambda_1 + 1 + \alpha_1)^2}{\left(1 + \frac{(-\lambda_1 + 1 + \alpha_1)^2 \epsilon}{\alpha_1^2}\right)^{3/2}} \alpha_1^2 - \frac{-\lambda_1(-\lambda_2 + 1 + \alpha_1)(-\lambda_1 + 1 + \alpha_1)}{\left(1 + \frac{(-\lambda_2 + 1 + \alpha_1)^2 \epsilon}{\alpha_1^2}\right) \alpha_1^2 \sqrt{1 + \frac{(-\lambda_1 + 1 + \alpha_1)^2 \epsilon}{\alpha_1^2}} (\lambda_1 - \lambda_2)} \\ -\frac{1}{2} \frac{(-\lambda_1 + 1 + \alpha_1)^3}{\left(1 + \frac{(-\lambda_1 + 1 + \alpha_1)^2 \epsilon}{\alpha_1^2}\right)^{3/2}} \alpha_1^3 - \frac{\lambda_1(-\lambda_2 + 1 + \alpha_1)^2(-\lambda_1 + 1 + \alpha_1)}{\left(1 + \frac{(-\lambda_2 + 1 + \alpha_1)^2 \epsilon}{\alpha_1^2}\right) \alpha_1^3 \sqrt{1 + \frac{(-\lambda_1 + 1 + \alpha_1)^2 \epsilon}{\alpha_1^2}} (\lambda_1 - \lambda_2)} \end{array} \right\} \quad (7)$$

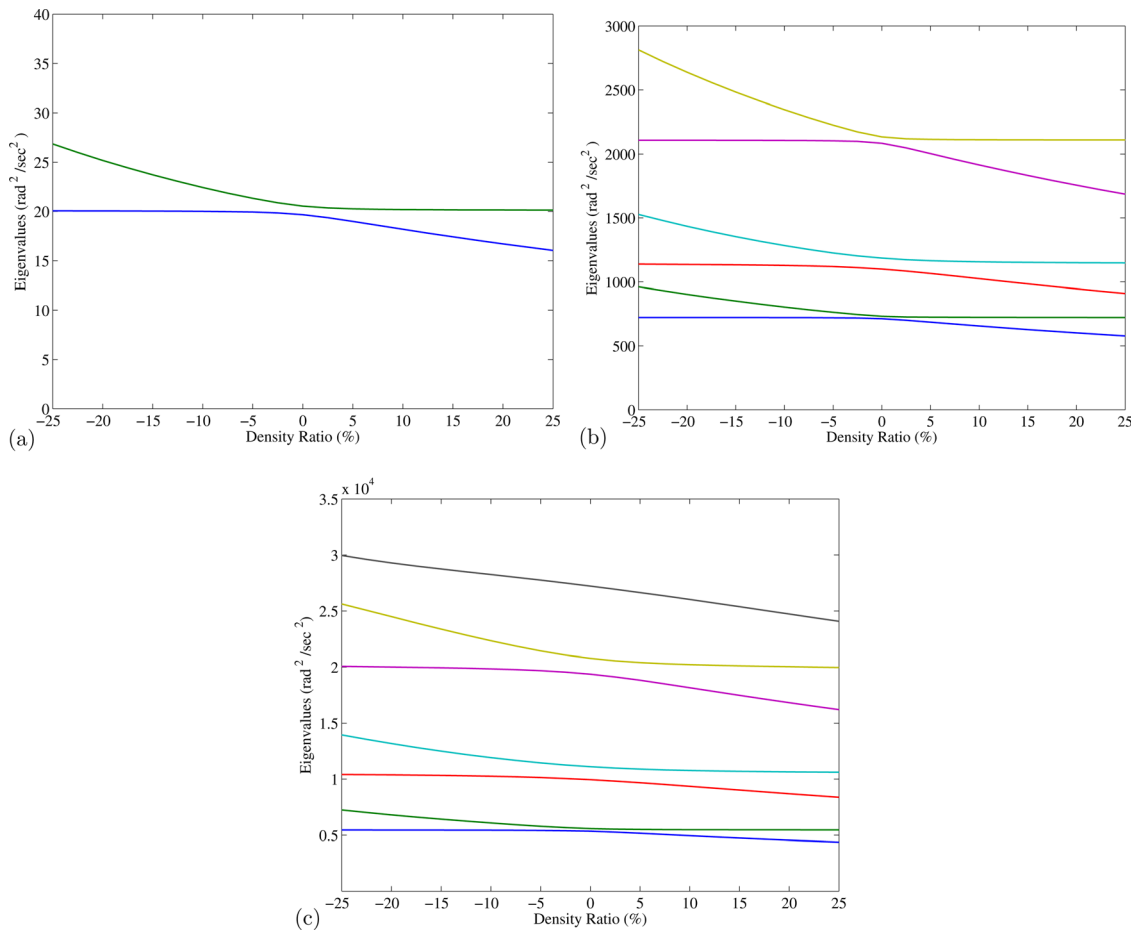


Fig. 3 Eigenvalue veering in a coupled beam system subjected to $\pm 25\%$ variation in mass density: (a) Modes 1 to 2, (b) Modes 3 to 8, and (c) Modes 9 to 15

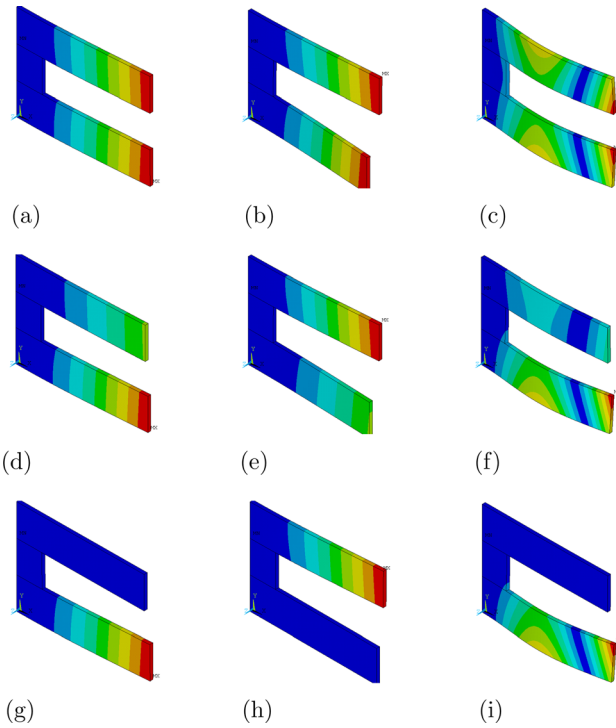


Fig. 4 Vibration modes of the coupled beam system subjected to variations in mass density of one beam: (a) Mode 1: 0%, (b) Mode 2: 0%, (c) Mode 3: 0%, (d) Mode 1: 2.5%, (e) Mode 2: 2.5%, (f) Mode 3: 2.5%, (g) Mode 1: 25%, (h) Mode 2: 25%, and (i) Mode 3: 25%

Thus, the derivative of Mode 1 is very sensitive to the spacing eigenvalues λ_1 and λ_2 . Systems with closely spaced eigenvalues are known to veer and Pierre [26] showed that mode localization strongly corresponds to eigenvalue veering. In the case of periodic structures, the perfect symmetry yields repeated eigenvalues, for example $\lambda_1 = \lambda_2$. However, in the presence of parametric

uncertainties the symmetry is broken and the repeating eigenvalues are split into distinct values [30–32]. This change in the eigenvector, due to some variation of the mass and stiffness matrices in the system, is what has to be quantified. In Sec. 3, we explain a possible way to achieve this.

3 Quantifying Localization Using the MAC

The MAC has been used extensively to compare experimental mode shapes to numerical mode shapes [22,25,33]. For the purpose of quantifying localization, the MAC is used to compare two numerical finite element models with identical number of degrees-of-freedom. The MAC is defined as

$$MAC_{ij} = \frac{(\mathbf{x}_i^T \mathbf{x}_j)^2}{(\mathbf{x}_i^T \mathbf{x}_i)(\mathbf{x}_j^T \mathbf{x}_j)} \quad (8)$$

where $i, j \in [1, 2, \dots, N]$ denote the mode numbers of the eigenvectors in a general system with N degrees-of-freedom. The non-localized eigenvectors obtained for $\epsilon = 1$ are denoted by \mathbf{b}_k . The proposed MACLF for Mode j of the N degrees-of-freedom system is

$$MACLF_j = \max_{1 \leq k \leq N} \left[\frac{(\mathbf{x}_i^T \mathbf{b}_k)^2}{(\mathbf{x}_i^T \mathbf{x}_i)(\mathbf{b}_k^T \mathbf{b}_k)} \right] \quad (9)$$

In parametric studies, one or more system properties are varied, and in such instances the numbering of the localized modes does not always correspond to the mode numbers of the system with nonlocalized modes. Complex dynamic systems such as coupled beam system in Sec. 4 and the bladed disk in Sec. 5 are prone to mode swapping. Physically pairing the corresponding modes are important for accurate correlation between modes to quantify localization, and hence the maximum MAC value is chosen to pair the correct modes.

In large systems, solving Eq. (1) each time to obtain the eigenvalues and eigenvectors for variations to the mass and stiffness matrices can be computationally expensive. By utilizing the well-

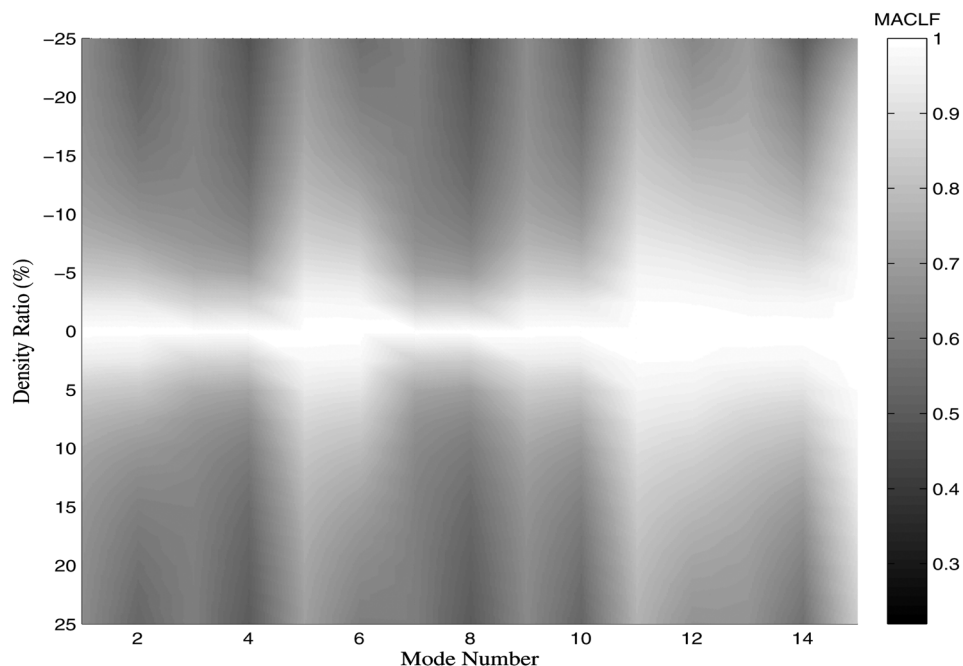


Fig. 5 MACLF applied to the coupled beam system for a variation of density in one beam

known first-order perturbation methods, eigenvalues and eigenvectors can be efficiently computed for the parametric study. Fox and Kapoor [27] developed a first-order expression to compute the derivatives of real eigenvalues and eigenvectors in systems with distinct eigenvalues. Mills-Curran [34] outlined a method to obtain the derivatives of repeated eigenvalues. Assuming that the derivatives of the eigenvalues are distinct, the derivatives of the eigenvectors may also be calculated [34]. By obtaining the eigenvalues, λ_k , and eigenvectors, ψ_k , for the unperturbed system, the eigensystem for other parameters can be estimated using the sensitivities of the eigenvalues and eigenvectors. It should be noted that the perturbation approach suggested for the system with

repeated modes work only when one parameter is varied [35]. The perturbed eigenvalues and eigenvectors for a parameter change of Δp are denoted by $\hat{\lambda}_k$ and $\hat{\psi}_k$, respectively, and are given by

$$\hat{\lambda}_k = \lambda_k + \frac{\partial \lambda_k}{\partial p} \Delta p \quad (10)$$

$$\hat{\psi}_k = \psi_k + \frac{\partial \psi_k}{\partial p} \Delta p \quad (11)$$

The MACLF for the j th Mode calculated using the sensitivity approach is denoted by MACLF_j , and may be computed with reduced computational effort. In Sec. 4, a two coupled cantilever

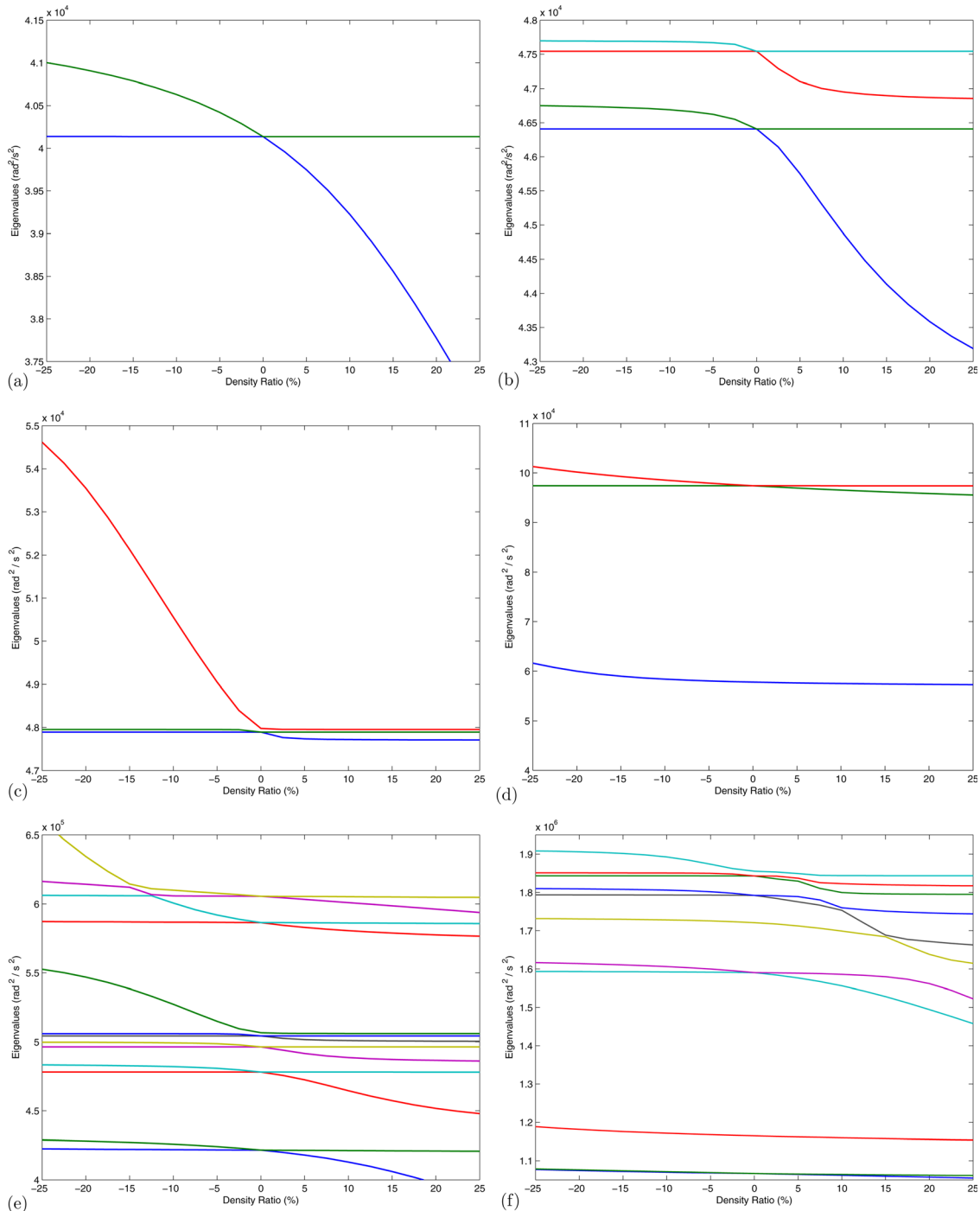


Fig. 6 Eigenvalues of the bladed disk system subjected to variations in the mass density of one blade: (a) Eigenvalues λ_1 : λ_2 ; (b) Eigenvalues λ_3 : λ_6 ; (c) Eigenvalues λ_7 : λ_9 ; (d) Eigenvalues λ_{10} : λ_{12} ; (e) Eigenvalues λ_{13} : λ_{25} ; and (f) Eigenvalues λ_{26} : λ_{36}

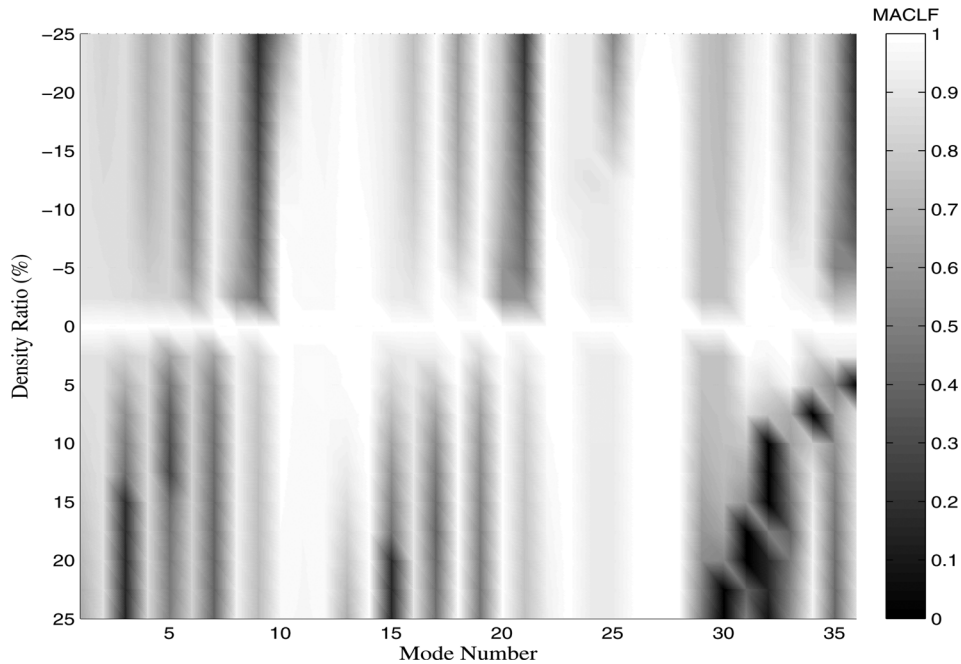


Fig. 7 MACLF for a bladed disk system for a variation in density

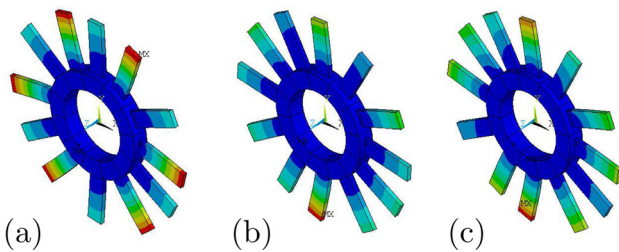


Fig. 8 Mode 15 of the bladed disk system subjected to variations in density of one blade: (a) Mode 15–0%, (b) Mode 15–2.5%, and (c) Mode 15–20%

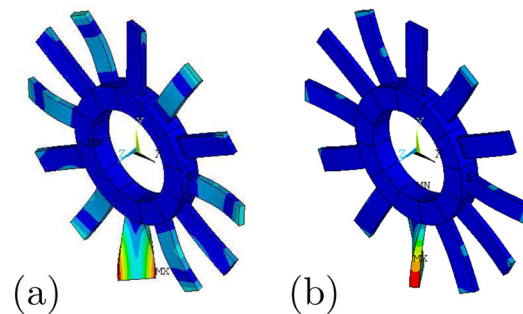


Fig. 10 Mode 31 exhibiting extreme localization: (a) Mode 31–20% and (b) Mode 31–15%

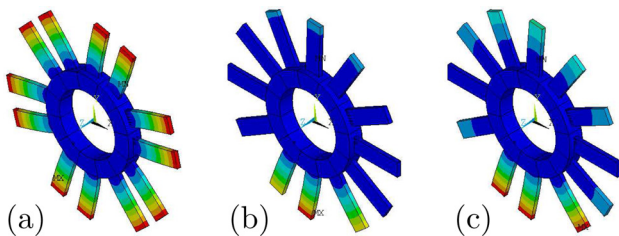


Fig. 9 Mode 21 of the bladed disk system subjected to variations in density of one blade: (a) Mode 21–0%, (b) Mode 21–10%, and (c) Mode 21–17.5%

beam system is used as an example to quantify localization in systems with distinct eigenvalues. A more complex bladed disk system with repeated eigenvalues is shown in Sec. 5.

4 Localization in a Coupled Beam System

A finite element model of the two coupled cantilever beam system was developed for this numerical experiment. The uncertainty was introduced in the form of varying the density of only one beam and the rest of the system was kept unchanged. The boundary condition of the system was fixed at one end throughout the parametric study. The first 15 eigenvectors of system were considered. The mass density of a single beam was varied by $\pm 25\%$ and

the resulting eigenvalues are shown in Fig. 3. The first three mode shapes and their sensitivity to variations in the mass density of a single beam are shown in Fig. 4. The unperturbed system is considered to be perfect and the vibrations are evenly distributed as seen in Figs. 4(a)–4(c). Varying the density by -2.5% changes the displacement of the two beams; one beam has notably less displacement than the other. This change in amplitude can be observed by comparing Figs. 4(a) and 4(d), 4(b) and 4(e), and 4(c) and 4(f). In the extreme case of a -25% variation in the mass density, the displacement of one beam is significantly lower than the other, this can be seen in Figs. 4(g)–4(i). The eigenvalues of the coupled beam system shown in Fig. 3 veer with the variation in mass density. Comparing Figs. 3 and 4 strengthens the claim that eigenvalue veering is closely associated with mode localization.

Figure 5 shows the MACLF for each mode for various mass density ratios using the method outlined in Eq. (9). As an example, the first three modes of the coupled beam system with no density variation are shown in Figs. 4(a)–4(c) which shows an MACLF of one. Figure 4 also shows the mode shapes for density variations of -2.5% and -25% as examples of perturbed systems. From Fig. 5, a density ratio of -2.5% gives an MACLF for the first three modes of approximately 0.75–0.85, indicating moderate localization. As an extreme case, the coupled beam system was perturbed with a -25% variation in density and MACLF values in

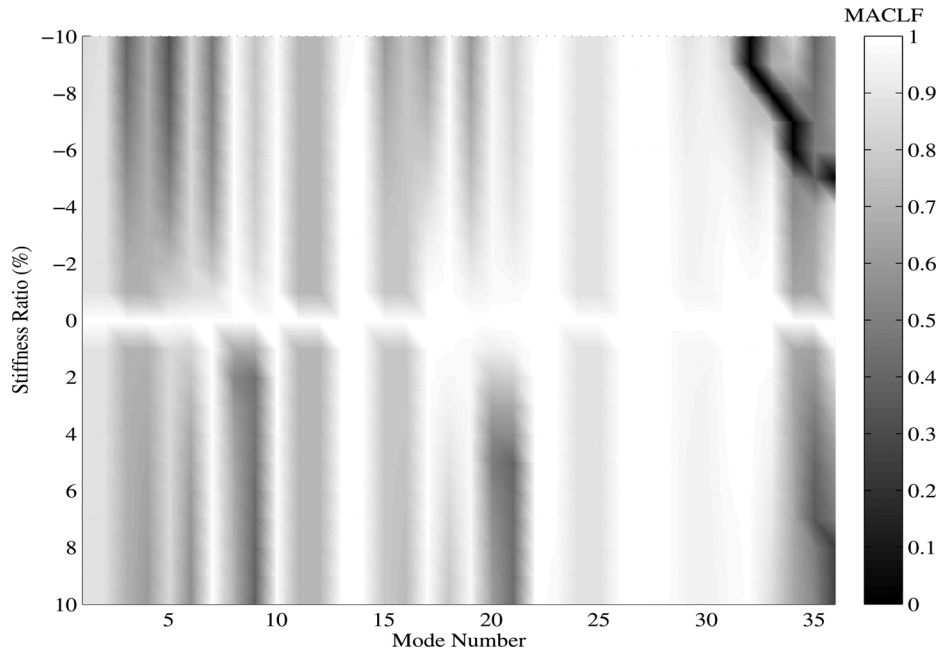


Fig. 11 The MACLF values for a bladed disk system for a variation in the stiffness of a single blade

the range of 0.45–0.6 were observed for the first three modes, including high localization.

The parametric study above solves the full eigenvalue problem to obtain the eigenvalues and eigenvectors for the different variations in density. The sensitivity approach could be utilized to efficiently compute the eigenvalues and eigenvectors of the subsequent states by solving Eq. (1) for the nonlocalized system. The method of Fox and Kapoor [27] was used to calculate the derivatives of the eigenvalues in Eq. (10) and the eigenvectors in Eq. (11). The expression for eigenvalue sensitivity for a variation in the mass distribution p is

$$\frac{\partial \lambda_j}{\partial p} = \psi_j^T \left[-\lambda_j \frac{\partial \mathbf{M}}{\partial p} \right] \psi_j, \quad \text{since} \quad \frac{\partial \mathbf{K}}{\partial p} = 0 \quad (12)$$

Thus, Fig. 3 can be obtained with reduced computational effort by using Eqs. (10) and (12). The eigenvector derivatives of the coupled beam system, with respect to a mass parameter p , are

$$\frac{\partial \psi_j}{\partial p} = -\frac{1}{2} \left(\psi_j^T \frac{\partial \mathbf{M}}{\partial p} \psi_j \right) \psi_j + \sum_{k=1, k \neq j}^N \frac{\psi_k^T \left[-\lambda_j \frac{\partial \mathbf{M}}{\partial p} \right] \psi_j}{\lambda_j - \lambda_k} \psi_k \quad (13)$$

The eigenvectors obtained using the sensitivities are denoted by $\hat{\psi}_j$. By using $\hat{\psi}_j$ and \mathbf{b}_k for the method outlined in Eq. (9), a plot similar to Fig. 5 can be obtained with reduced computational effort by using the sensitivity approach ($\hat{m}_j \approx m_k$).

5 Localization in Bladed Disks

For this numerical study, a finite element model of the idealized bladed disk was developed, using 8-noded solid brick elements with 12 sectors, 12 blades with 294,912 degrees-of-freedom. The number of degrees-of-freedom was kept constant and the bladed disk was modeled free–free. Two numerical studies were performed on the bladed disk system: varying the mass density of one blade within the range $\pm 25\%$ and varying the stiffness of one blade by varying the Young’s modulus within the range $\pm 10\%$. The MACLF values are calculated and then evaluated by comparing to the eigenvalue veering regions and by visually inspecting the modes of vibration. A sensitivity-based approach is proposed

to calculate the eigenvalues and eigenvectors with reduced computational effort.

5.1 Variability in the Mass Distribution. The variation in the eigenvalues, as the mass density of a single blade varies by $\pm 25\%$, is shown in Fig. 6. The eigenvalues were obtained by solving the full eigenvalue problem for each variation in mass density, although the eigenvalues could be computed using the sensitivity approach. Note that the bladed disk system possesses repeated eigenvalues when there is no variation in mass density, and hence the method of Fox and Kapoor [27] will not work. Mills-Curren [34] gave a method to calculate the eigenvalue and eigenvector derivatives of systems with repeated eigenvalues, provided the repeated eigenvalues possess distinct derivatives.

The MACLF plot for the variability in mass density is shown in Fig. 7. The MACLF results should be compared to the curve veering regions in Fig. 6, and with example mode shapes given in Figs. 8 and 9. The curve veering regions always correspond to localized modes and in extreme curve veering the modes are also seen to be severely affected. For example, in Fig. 6(e) the 15th Mode is seen to veer, and Fig. 7 shows that the MACLF has values of approximately 1, 0.45, and 0.25 for 0%, 2.5%, and 20% variations in the mass density. Mode 21, shown in Fig. 8, has MACLF values of approximately 1, 0.35, and 0.15 for 0%, -10% , and -17.5% variations in the mass density. Hence, the MACLF accurately quantifies the degree of localization due to various perturbations in mass density. Observing the darker areas in Fig. 7

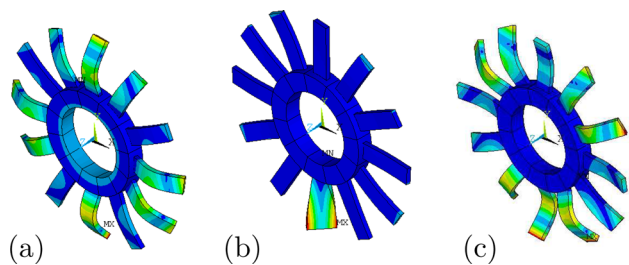


Fig. 12 Modes with a -10% variation in the Young’s modulus of a single blade: (a) Mode 31– 10% , (b) Mode 32– 10% , and (c) Mode 33– 10%

corresponding to MACLF values in the range of 0–0.1 shows that the vibrations are confined mostly to one blade. Examples of such extreme localization can be seen in Mode 31 for density ratios of –20% and –15% given in Fig. 10. In Fig. 6(f), the eigenvalue for Mode 31 rapidly veers for density ratio of 15% upward. Hence, MACLF values indicate different levels of localization, and for the purpose of quantifying localization they can be categorized into three groups. Vibration modes with minimum or no localization generates MACLF values around 0.7 to 1, modes with moderate localization always possess MACLF values around 0.4–0.6, and for any MACLF values below 0.3 the modes are severely localized.

5.2 Variability in the Stiffness Distribution. This section focuses on disturbing the stiffness distribution by varying the Young’s modulus of a single blade and then quantifying the localization in vibration modes using the MACLF. The first 36 modes of the system with a $\pm 10\%$ variation in Young’s modulus were considered for this study. The Taylor series and sensitivity expression can be utilized to compute the eigenvectors for the parametric study, using Eqs. (10) and (11), and then the MACLF is obtained using Eq. (9). Figure 11 shows the MACLF plot for the 36 modes, and highlights that some of the modes are insensitive to localization due to parametric uncertainties. It can be observed from Figs. 7 and 11 that the nonlocalized modes 14, 23, 26, 27, and 28 are not sensitive to changes to the mass or stiffness distribution of the

blades. A similar pattern of MACLF values generated by the previous study in Fig. 7 is also observed in Fig. 11. The degree of localization can be categorized into three different cases. Case 1 with the MACLF values are between 0.6 and 1.0 indicating minimum or no localization, case 2 with MACLF between 0.2 and 0.6 indicating moderate localization, and case 3 with MACLF between 0 and 0.2 indicating strong localization. Figure 12 highlights the three different categories of localization.

5.3 The Effect of Noise in the Modal Data. The MACLF can also be applied to experimental data to quantify localization and to simulate a physical experiment, and the numerical modal data were corrupted with noise. As an example, the system with –10% stiffness reduction was corrupted with 10% and 20% noise. High levels of random noise are used to explore the robustness of the method. The “measured” eigenvectors are

$$\tilde{\mathbf{x}}_j = \mathbf{x}_j(1 + \alpha\beta_j) \quad (14)$$

$$\tilde{\mathbf{b}}_k = \mathbf{b}_k(1 + \alpha\beta_k) \quad (15)$$

where $\tilde{\mathbf{x}}_j$ and \mathbf{b}_k are the eigenvectors of the nonperfect and perfect systems with the added noise. Here α is the percentage of added noise and β is the random vector generated from a zero mean, unit variance Gaussian distribution. Figure 13(a) shows the MACLF for the noiseless data, and Figs. 13(b) and 13(c) show the MACLF

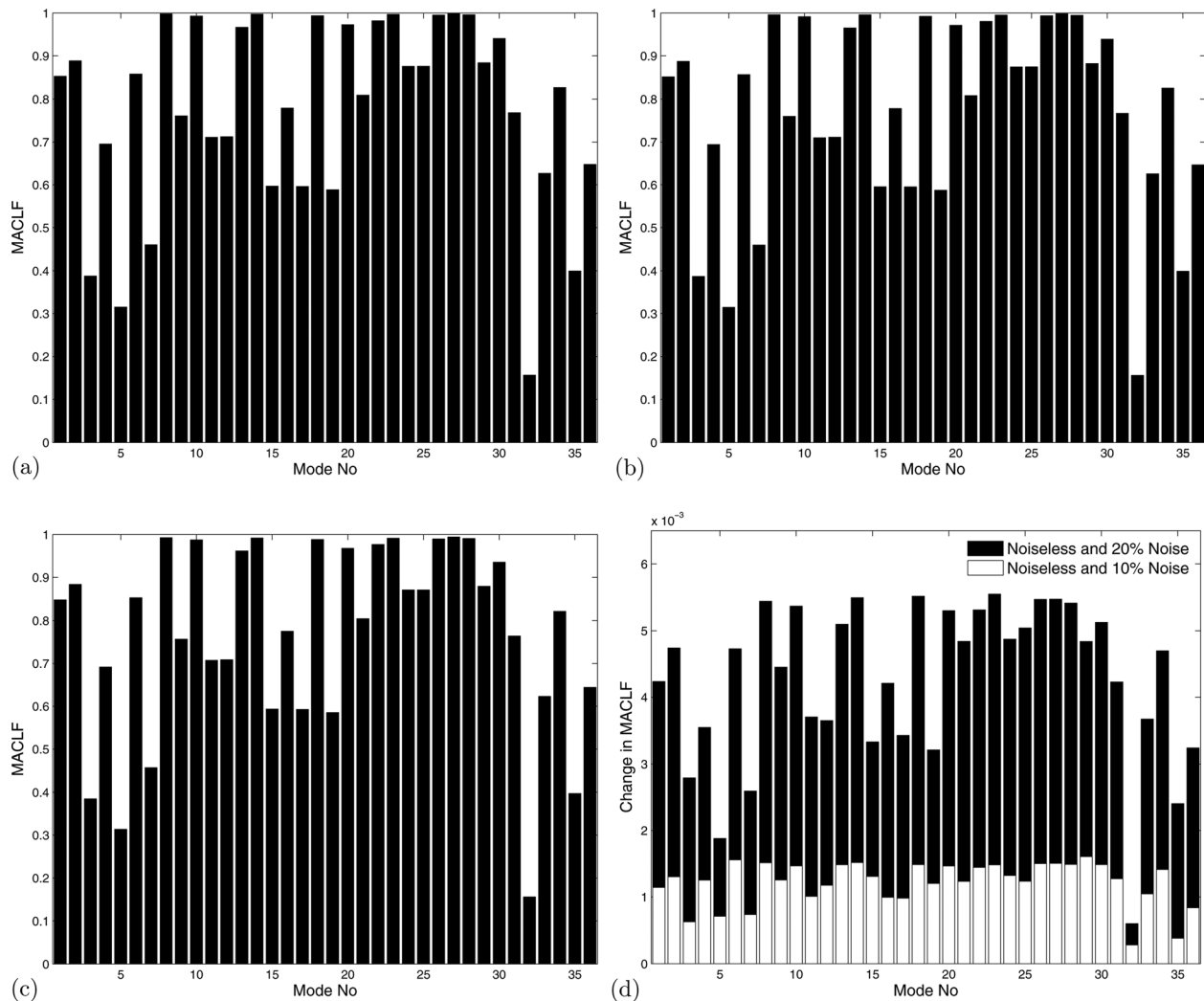


Fig. 13 Modes with a –10% variation in the Young’s modulus of a single blade: (a) MACLF with no noise, (b) MACLF with 10% noise, (c) MACLF with 20% noise, and (d) Change in MACLF for different strengths in noise

values when noise is added. The addition of numerical noise does not significantly alter the MACLF values. Figure 13(d) compares the change in MACLF between the example with no noise, 10% noise, and 20% noise for a bladed disk system subjected to -10% reduction in Young's modulus of a single blade. The MACLF in the presence of moderate noise can predict the localized modes to a good degree of accuracy.

6 Conclusions

A numerical method has been proposed to identify and quantify mode localization in periodic structures. The MAC across all the modes due to the changes in some system parameters has been exploited. A value between 0 and 1 is given by the proposed MACLF, where 1 indicates no localization and 0 indicates the highest possible localization. Any value between 0 and 1 can be interpreted as the degree of mode localization. Only the modal data, that is the natural frequencies and mode shapes, are necessary to apply this approach. For purely numerical computation of MACLF, a first-order perturbation based approach using the modal sensitivities has been suggested.

The idea behind the proposed MACLF was explored using three numerical examples with progressive complexity, namely, a 2DOF discrete system, a coupled-beam system, and a bladed disk with 12 blades. The study was conducted by perturbing the mass or stiffness distribution, and the results were verified with eigenvalue veering and mode shape plots. For periodic structures, MACLF values in the range of 0.6–1.0 indicate minimal localization, and values in the ranges 0.6–0.2 and 0.0–0.2 indicate moderate and extreme localization, respectively. To simulate real experiments, the modal data were corrupted by random noise with various strengths. It was observed that the MACLF values still predict the localized modes with reasonable accuracy even for 20% noise. The investigation is restricted to undamped linear dynamical systems. In the future, the proposed method will be investigated for nonproportionally damped systems possessing complex modes.

References

- [1] Hart, J. D., Ford, G. W., and Saure, R., 1992, "Mitigation of Wind Induced Vibration of Arctic Pipeline Systems," ASME 11th International Conference on Offshore Mechanics and Arctic Engineering, Calgary, AB, Canada, June 7–12.
- [2] Castanier, M. P., and Pierre, C., 2006, "Modeling and Analysis of Mistuned Bladed Disk Vibration: Status and Emerging Directions," *J. Propul. Power*, **22**(2), pp. 384–396.
- [3] Nikolic, M., 2006, "New Insights into the Blade Mistuning Problem," Ph.D. thesis, Imperial College, London.
- [4] Nikolic, M., Petrov, E. P., and Ewins, D. J., 2008, "Robust Strategies for Forced Response Reduction of Bladed Disks Based on Large Mistuning Concept," *ASME J. Eng. Gas Turbines Power*, **130**(2), pp. 285–295.
- [5] Blair, A. J., 1997, "A Design Strategy for Preventing High Cycle Fatigue by Minimising Sensitivity of Bladed Disks to Mistuning," Master's thesis, Wright State University, Dayton, OH.
- [6] Chen, Y. F., and Shen, I. Y., 2015, "Mathematical Insights Into Linear Mode Localization in Nearly Cyclic Symmetric Rotors With Mistune," *ASME J. Vib. Acoust.*, **137**(4), p. 041007.
- [7] Pestel, E. C., and Leckie, F. A., 1963, *Matrix Methods in Elastomechanics*, McGraw-Hill, New York.
- [8] Soong, T. T., and Bogdanoff, J. L., 1963, "On the Natural Frequencies of a Disordered Linear Chain of n Degrees of Freedom," *Int. J. Mech. Sci.*, **6**(3), pp. 225–237.
- [9] Lin, Y. K., and Yang, J. N., 1974, "Free Vibration of a Disordered Periodic Beam," *ASME J. Appl. Mech.*, **41**(2), pp. 383–391.
- [10] Yang, J. N., and Lin, Y. K., 1975, "Frequency Response Functions of a Disordered Periodic Beam," *J. Sound Vib.*, **38**(3), pp. 317–340.
- [11] Kissel, G. J., 1988, "Localization in Disordered Periodic Structures," Ph.D. thesis, MIT, Boston.
- [12] Kissel, G. J., 1992, "Localization Factor for Multichannel Disordered Systems," *Phys. Rev. A*, **44**(2), pp. 1008–1014.
- [13] Lin, Y. K., and Cai, G. Q., 1991, *Disordered Periodic Structures*, Springer, Dordrecht, The Netherlands.
- [14] Lin, Y. K., and Cai, G. Q., 1995, *Probabilistic Structural Dynamics*, McGraw-Hill, New York.
- [15] Xie, W. C., and Ariaratnam, S. T., 1994, "Numerical Computation of Wave Localization in Large Disordered Beamlike Lattice Trusses," *AIAA J.*, **32**(8), pp. 1724–1732.
- [16] Xie, W. C., and Ariaratnam, S. T., 1996, "Vibration Mode Localization in Disordered Cyclic Structures: Single Substructure Mode," *J. Sound Vib.*, **189**(5), pp. 625–645.
- [17] Xie, W. C., and Ariaratnam, S. T., 1996, "Vibration Mode Localization in Disordered Cyclic Structures: Single Substructure Mode," *J. Sound Vib.*, **189**(5), pp. 647–660.
- [18] Ariaratnam, S. T., and Xie, W. C., 1995, "Wave Localization in Randomly Disordered Nearly Periodic Long Continuous Beams," *J. Sound Vib.*, **181**(1), pp. 7–22.
- [19] Fang, Z., 1995, "Dynamic Analysis of Structures With Uncertain Parameters Using the Transfer Matrix Method," *Comput. Struct.*, **55**(6), pp. 1037–1044.
- [20] Mitchell, T. P., and Moini, H. A., 1992, "An Algorithm for Finding the Natural Frequencies of a Randomly Supported String," *Probab. Eng. Mech.*, **7**(1), pp. 23–26.
- [21] Langley, R. S., 1996, "A Transfer Matrix Analysis of the Energetics of Structural Wave Motion and Harmonic Vibration," *Proc. R. Soc. Ser. A*, **452**(1950), pp. 1631–1648.
- [22] du Bois, J. L., Adhikari, S., and Lieven, N. A. J., 2009, "Mode Veering in Stressed Framed Structures," *J. Sound Vib.*, **322**(4–5), pp. 1117–1124.
- [23] Liu, X. L., 2002, "Behaviour of Derivatives of Eigenvalues and Eigenvectors in Curve Veering and Mode Localization and Their Relation to Close Eigenvalues," *J. Sound Vib.*, **256**(3), pp. 551–564.
- [24] du Bois, J. L., Adhikari, S., and Lieven, N. A. J., 2011, "On the Quantification of Eigenvalue Curve Veering: A Veering Index," *ASME J. Appl. Mech.*, **78**(4), p. 041007.
- [25] Allemang, R. J., 2003, "The Modal Assurance Criterion - Twenty Years of Use and Abuse," *Sound Vib.*, **37**(8), pp. 14–23.
- [26] Pierre, C., 1988, "Mode Localization and Eigenvalue Loci Veering Phenomena in Disordered Structures," *J. Sound Vib.*, **126**(3), pp. 485–502.
- [27] Fox, R. L., and Kapoor, M. P., 1968, "Rates of Change of Eigenvalues and Eigenvectors," *AIAA J.*, **6**(12), pp. 2426–2429.
- [28] Adhikari, S., 2000, "Calculation of Derivative of Complex Modes Using Classical Normal Modes," *Comput. Struct.*, **77**(6), pp. 625–633.
- [29] Adhikari, S., 2001, "Eigenrelations for Non-Viscously Damped Systems," *AIAA J.*, **39**(8), pp. 1624–1630.
- [30] Rao, J. S., 2006, "Mistuning of Bladed Disk Assemblies to Mitigate Resonance," *Adv. Vib. Eng.*, **5**(1), pp. 17–24.
- [31] Vijayan, K., and Woodhouse, J., 2014, "Shock Transmission in a Coupled Beam System," *J. Sound Vib.*, **333**(5), pp. 1379–1389.
- [32] Vijayan, K., and Woodhouse, J., 2013, "Shock Transmission in a Coupled Beam System," *J. Sound Vib.*, **332**(16), pp. 3681–3695.
- [33] Friswell, M. I., and Mottershead, J. E., 1999, *Finite Element Model Updating in Structural Dynamics*, Kluwer Academic Publishers, UK.
- [34] Mills-Curran, W. C., 1988, "Calculation of Eigenvector Derivatives for Structures With Repeated Eigenvalues," *AIAA J.*, **26**(7), pp. 867–871.
- [35] Friswell, M. I., 1996, "The Derivatives of Repeated Eigenvalues and Their Associated Eigenvectors," *ASME J. Vib. Acoust.*, **118**(3), pp. 390–397.